



High Temperature Schottky Barrier on *n*-Type SrTiO₃ and Its Sensitivity to Ambient Gases

T. KAWADA,* T. ICHIKAWA, L.Q. HAN, K. YASHIRO, H. MATSUMOTO & J. MIZUSAKI

Institute of Multidisciplinary Research for Advanced Materials, Tohoku University, 2-1-1 Katahira, Aoba-ku, Sendai 980-8577, Japan

Submitted March 4, 2003; Revised February 2, 2004; Accepted February 3, 2004

Abstract. Metal or oxide electrodes (Pt, Au, Ag, (La,Sr)CoO₃) were deposited on single crystals of 0.02 mol% Nb doped SrTiO₃ by pulsed laser deposition. Current-voltage and capacitance-voltage responses were measured using three-terminal electrode configuration. Under high oxygen partial pressures, clear rectification behaviors were observed. Diffusion model well explained the current vs. voltage relationship with ideality factors close to unity. The barrier height varied reversibly with oxygen partial pressure, and was almost independent of the electrode materials, which suggested that the Fermi level at the interface was pinned by the surface states. The origin of the surface states was discussed in terms of oxygen adsorption or oxidative formation of metal vacancies around the surface. Chemical interaction between the surface and oxygen and resulting cation rearrangement was concluded to play an important role from the long stabilization time on oxygen partial pressure change. The water vapor pressure dependence of the barrier height was also explained by competitive adsorption of oxygen and water.

Keywords: SrTiO₃, Schottky barrier, high temperature, water, interface

Introduction

Strontium titanate or barium titanate based perovskites are widely used in electronic devices such as capacitors, FeRAMs, PTCR thermistors, varistors, etc. They are also attractive for high temperature applications like resistance gas sensors or high temperature fuel cells. Titanate perovskites show high stability over wide range of oxygen partial pressure and temperature. The electronic properties, however, varies drastically with the atmosphere. The main charge carrier can be electron, hole, oxide ion or proton depending on the dopant cations, ambient gases, and temperature. Although the bulk transport behaviors are well described in terms of defect chemistry, interface properties are not simple. In most applications, control of electron transfer at the interfaces is a key issue. An enormous number of studies have been reported on the characterization and modification of the interfaces. So far, however, high temperature behaviors of the interface have not been

clarified enough. For donor doped SrTiO₃, the grain boundary or the surface are known to have much higher resistance than the bulk [1–9]. Niobium segregation, Sr vacancy and/or Sr_{*n*+1}Ti_{*n*}O_{3*n*+1} phase formation, or Schottky barrier have been considered in the literatures as the reason of the high resistivity. The present authors have reported that the interface between platinum and 1 mol% Nb doped SrTiO₃ exhibits Schottky barrier type rectification behavior even at high temperatures as 600°C [9]. The barrier height reversibly varied with the partial pressure of ambient oxygen. In a recent experiment, an ideal Schottky contact was obtained at the interface of platinum and SrTiO₃ with less Nb concentration. In this paper, the results of high temperature *I*-*V* and *C*-*V* measurements are presented, and their sensitivity to ambient gases (oxygen and humidity) is discussed.

Experimental

Single crystals of strontium titanate doped with nominally 0.01 wt.% niobium (~0.02 mol%, STNO), was

*To whom all correspondence should be addressed. E-mail: kawada@tagen.tohoku.ac.jp

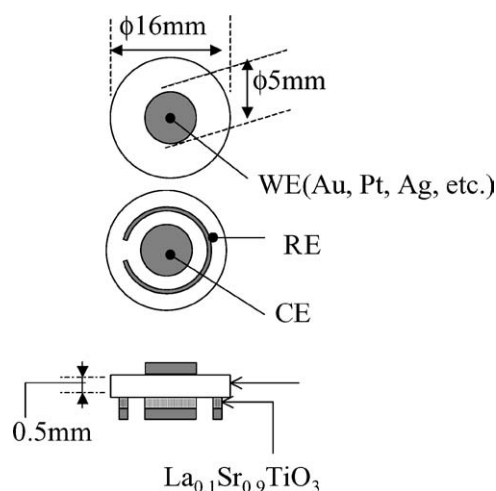


Fig. 1. Schematic view of the electrode configuration on the samples.

purchased from Nakazumi crystal Co. The crystal size was 0.5 mm in thickness and 15 mm in diameter, with polished (1 0 0) surfaces. Metal or oxide electrodes, Pt, Au, Ag, $\text{La}_{0.6}\text{Sr}_{0.4}\text{CoO}_3$, and $(\text{Sn}_{0.905}\text{In}_{0.095})\text{O}_2$, were deposited on the center of the pellet by pulsed laser deposition as the working electrode (WE). The substrate, STNO, was heated at 873 K during the deposition. Ultraviolet laser light (Ar-F or Xe-Cl) irradiated a rotating target disk with the incident angle of 45 degree and repetition rate, 5 Hz. The resulting electrode thickness was around 500 Å. A platinum counter electrode (CE) and a reference electrode (RE) were deposited on the opposite side of WE on the pellet. A thin layer of $\text{La}_{0.1}\text{Sr}_{0.9}\text{TiO}_3$ was deposited in advance in order to reduce the interface resistance. Current was flown through the sample between WE and CE, and the potential difference between WE and RE was monitored (Fig. 1). The measurements were carried out at the temperatures from 673 K to 873 K. The highest temperature was limited at 873 K so as not to make the electrode metals agglomerate or vaporize. For the measurements in oxidizing conditions, oxygen and argon mixed gases were flown at a flow rate of 20 ml/min. For comparison, 1% hydrogen - argon mixture saturated with water vapor at room temperature was flown in order to make a reducing atmosphere. For gas sensitivity tests, the composition of the gas was suddenly changed, and the interface resistance of the sample was monitored by ac measurements.

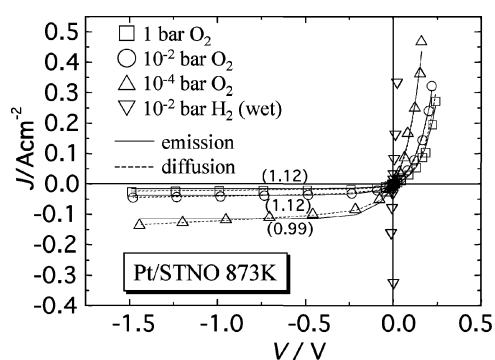


Fig. 2. Oxygen partial pressure dependence of current vs. voltage curves of the Pt/STNO interface at high temperature (873 K).

Results and Discussion

Interface Resistance

Figure 2 shows typical current-voltage behaviors of Pt/STNO interface at 873 K under various oxygen partial pressures. Under highly reducing atmospheres (humidified hydrogen), the interface resistance was small compared to the bulk resistance, and the I-V relation was linear. When it was annealed in oxygen containing gases, the interface resistance increased, and a rectification behavior appeared. Similar results were obtained also in our previous studies on the Pt/STNO interface with higher Nb concentration (1 mol%) [9]. In that case, however, a significant leak current was observed in the reverse bias. In contrast, the present results with lower Nb concentration (0.02 mol%) showed lower leak current.

Rectification behavior at the electrode/semiconductor interface is a characteristic feature of a Schottky diode. The electron transfer across the barrier takes place via thermionic emission or diffusion mechanism depending on the thickness of the depletion layer. The current-voltage curve is described as the Eqs (1) and (2) for the respective mechanisms [10].

emission

$$J = J_{\text{ST}} \left[\exp \left(\frac{qV}{\alpha k_{\text{B}} T} \right) - 1 \right] \quad (1)$$

$$J_{\text{ST}} = A^* T^2 \exp \left(- \frac{q\phi_{\text{B}}}{k_{\text{B}} T} \right)$$

diffusion

$$J = J_{SD} \left[\exp \left(\frac{qV}{\alpha k_B T} \right) - 1 \right]$$

$$J_{SD} = \left\{ \frac{q D_n N_c}{k_B T} \left[\frac{2q(V_D - V)N_D}{\epsilon_0 \epsilon_s} \right]^{\frac{1}{2}} \exp \left(-\frac{q\phi_B}{k_B T} \right) \right\} \quad (2)$$

A^* : effective Recharldson factor, ϕ_B : barrier height
 D : diffusion coefficient of electron, V_D : diffusion potential, N_D : donor density and N_c : effective density of state of conduction band, ϵ : permittivity of STNO.

In both cases, “ α ” denotes the ideality factor that is unity when the ideal Schottky barrier is formed. As shown in Fig. 2, the experimental data fitted well to those equations. The best fit results are represented by the solid and dotted lines for the emission and diffusion mechanisms, respectively. The diffusion model fitted better the results especially under the reverse bias. The numbers shown in the parentheses are the ideality factors when the diffusion model is applied. In most cases, the ideality factors were close to unity. Figure 3 shows the results of ac response measurements. The inductive loops observed at the high frequency range were independent of the sample and measurement conditions, and were attributed to the impedance of the equipment or the wiring. After it was subtracted, the remaining part was a single semicircle that was represented by a parallel resistance and capacitance. The resistance increased, and the capacitance decreased with increasing

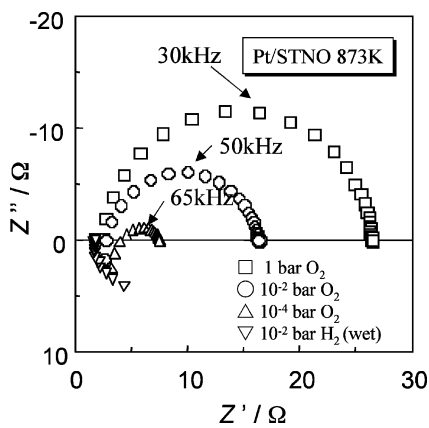


Fig. 3. Typical complex impedance plot for the Pt/STNO interface at 873 K.

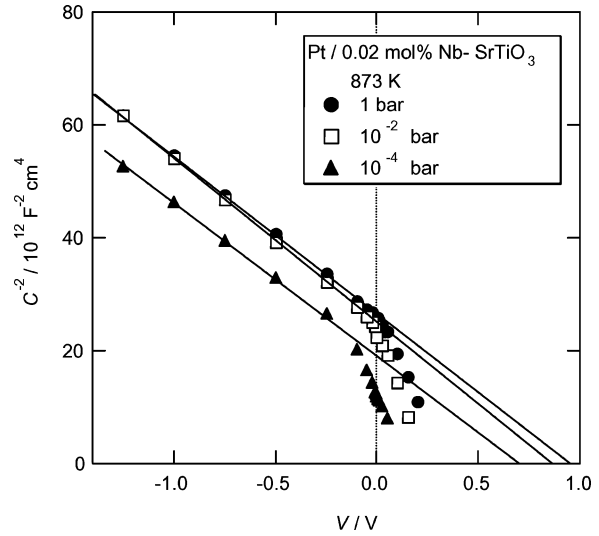


Fig. 4. Relationship between the interface capacitance and the applied potential for the Pt/STNO interface at 873 K.

negative bias potential as is expected for a depletion layer capacitance of a Schottky barrier. For a Schottky barrier, the capacitance is represented as Eq. (3) assuming a plane capacitor for the depletion layer [10].

$$C^{-2} = \frac{2}{e N_D \epsilon_s S^2} (V_D - V), \quad (3)$$

The C^{-2} against V plot showed a straight line (Fig. 4) as predicted from Eq. (3) at the inverse bias region. The increase in capacitance around the zero bias might be due to the surface states, which will be discussed later. The similar results were obtained with gold and silver electrodes, and even with oxide electrodes such as (La,Sr)CoO₃ or (Sn,In)O₂. Furthermore, in our preliminary experiments, the ITO/STNO interface showed photoresponse at 873 K, which confirms the existence of space charge layer at the temperature. Consequently, it is concluded that the Nb 0.02 mol% doped SrTiO₃ forms an ideal Schottky barrier with the electrodes even at elevated temperatures as 873 K.

Sensitivity to Oxygen

As shown in Figs. 2 and 3, interface resistance was dependent on oxygen partial pressure. Higher oxygen partial pressure caused higher resistance. The diffusion potential V_d estimated from the C^{-2} vs. V plot was

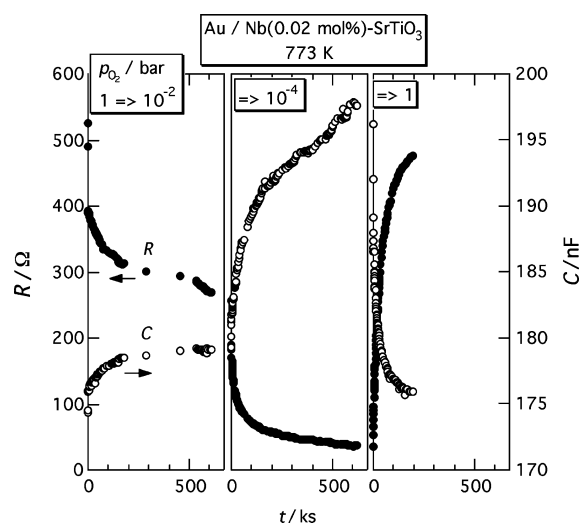


Fig. 5. Transient behavior of the resistance and capacitance of Au/STNO interface when oxygen partial pressure is varied at 773 K.

0.95 V, 0.84 V, and 0.77 V in oxygen partial pressures 1 bar, 10^{-2} bar, and 10^{-4} bar, respectively. The oxygen partial pressure dependence was similar among the samples with different electrodes although the absolute value of the barrier height was slightly dependent on the electrode material. The change was reversible in the oxidation and the reduction runs. Figure 5 shows the variation in the interface resistance and capacitance on a sudden change in the oxygen partial pressure for Au/STNO. The transition time, however, was rather long. It took more than hundred hours to reach a steady state. The factors that determine the equilibration time can be oxygen transport rate through the electrode layer and/or surface reaction rate. If oxygen transport predominated the kinetics, the relaxation time would have been dependent on the electrode material and the morphology. In the present experiments, no clear dependence on the electrode material was observed. The transition time was long even with (La,Sr)CoO₃ that is known as a good mixed conductor of electron and oxide ion. This suggests that the slow kinetics is not due to the oxygen transport but due to some chemical reaction that takes place at the STNO surface.

The origin of the Schottky barrier formation is discussed in terms of two extreme cases, i.e. Schottky limit and Bardeen limit. In the former case, the barrier height is determined by the difference between the work function of the electrode metal and the electron affinity of the semiconductor, whereas in the latter case, the barrier height is not dependent on the electrode but is fixed

at the surface level of the semiconductor. Robertson summarized the literature data on Schottky barrier at metal/SrTiO₃ interface measured at room temperature [11]. The reported data, however, are scattered since the sample preparation condition are quite different among the authors. For example, Shimizu et al. pretreated single crystals of Nb-SrTiO₃ by chemical etching and the succeeding ozone cleaning at elevated temperatures, and reported that the barrier was well explained by the Schottky limit [2]. The ozone treatment makes the surface of the sample in a highly oxidized state. It was probably kept unchanged during their measurements at room temperature. In contrast, our measurements were carried out in an equilibrium state at least for the surface of the sample. The surface state varies with the surrounding atmosphere not only in the pretreatment but also in the measurement conditions.

Table 1 summarizes the diffusion potentials determined from C^{-2} vs. V plot for various electrodes and oxygen partial pressure. The Schottky barrier observed in this study showed less dependence on the electrode materials than expected from the work function. It varied reversibly with varying oxygen partial pressure. Those results suggest that the Fermi level pinning at the interface dominates the barrier formation mechanism, i.e. it is close to Bardeen limit. One of the possible reasons for the formation of the surface states is oxygen adsorption. The Fermi level pinning by adsorbed oxygen was recently discussed in a quantitative way for SnO₂ by Rothschild and Komem [12]. The oxygen partial pressure dependence of the Schottky barrier in the present study is similar to that expected from their model. Another possible explanation is oxidative

Table 1. Effect of oxygen partial pressure and the electrode material on diffusion potential at electrode/SrTi_{0.9998}Nb_{0.0002}O₃ interface determined from C^{-2} vs. V plot at 873 K.

	V_D (V)		
	$p(\text{O}_2) = 1 \text{ bar}$	$p(\text{O}_2) = 10^{-2} \text{ bar}$	$p(\text{O}_2) = 10^{-4} \text{ bar}$
Au			
873 K	0.56	0.58	0.27
773 K	0.90	0.89	0.58
Pt			
873 K	0.95	0.84	0.77
773 K	0.90	0.89	0.58
(La,Sr)CoO ₃ ,			
873 K	0.85	0.85	0.74
773 K	1.00	0.99	0.94

formation of metal vacancies around the surface. Although single crystalline Nb-SrTiO₃ shows stable bulk conductivity even under 1 atm oxygen at elevated temperatures [13], the surface may be oxidized to form Sr vacancy that compensates the donor as reported by Moos and Härdtl for La doped SrTiO₃ [1]. Recently, Han et al. studied the surface of STNO annealed at 1273 K, and found that it consists of a double layer of (1) highly resistive thin surface skin of about 10 nm, which traps electrons, and (2) the resulting space charge layer (depletion layer) which dominates the electron transport resistance across the interface [14]. They mentioned the possibility of Sr vacancy formation accompanied by Ti-site substitution by Sr to explain the electron trapping at the surface skin. The similar kinetics can explain the present results. The surface skin layer, in the present case, must be very thin since its resistance was not detectable. The long relaxation time shown in Fig. 5 can be explained well by the slow kinetics of the cation transport and rearrangement.

Sensitivity to Water Vapor

Interface resistance and capacitance also varied with water vapor pressure. Figure 6 shows the transient behaviors when water vapor pressure is varied on Au/STNO interface. Resistance decreased and capacitance increased with increasing water vapor. This con-

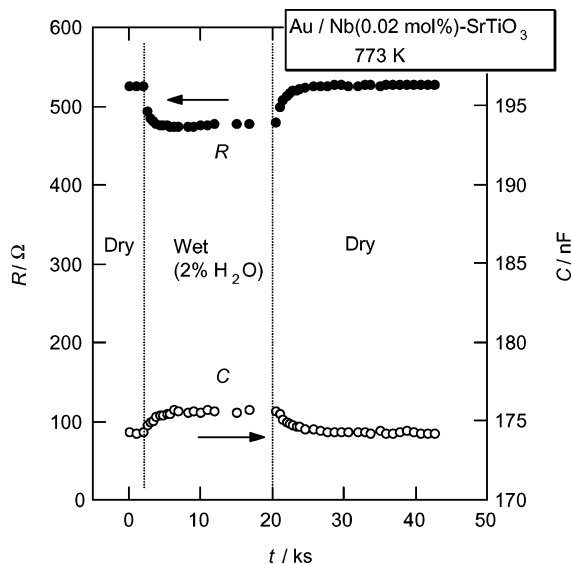


Fig. 6. Dependence on water vapor pressure on the resistance and capacitance of Au/STNO interface at 773 K under 1 bar oxygen.

firms that the surface level is an important factor to determine the high temperature Schottky barrier. In this case, however, the relaxation time was faster than that observed in the oxygen partial pressure perturbation by an order of magnitude. Dependences on the oxygen partial pressure and water vapor pressure can be based on different kinetics. The latter may be chemisorption of water on the surface or dissolution of proton in the surface layer, which are not accompanied by rearrangement of the constituent cations.

The properties of the surface layer on STNO should be clarified for further discussion.

Conclusion

An ideal Schottky barrier was formed between Nb 0.02 mol%-SrTiO₃ and metal or oxide electrodes even at elevated temperatures as 673 to 873 K. The barrier height was positively dependent on oxygen partial pressure. The change was reversible but had long transition time. Introduction of water vapor decreased the barrier height. The Schottky barrier formation mechanism was close to Bardeen's limit.

References

1. R. Moos and K.H. Härdtl, *J. Am. Ceram. Soc.*, **80**, 2549 (1997).
2. T. Shimizu, N. Gotoh, N. Shinozaki, and H. Okushi, *Appl. Surf. Sci.*, **117/118**, 400 (1997).
3. J. Sheng, K. Masuda, and T. Fukami, *J. Mater. Sci. Lett.* **16**, 2036 (1997).
4. S.-H. Kim, J.-H. Moon, J.-H. Park, J.-G. Park, and Y. Kim, *J. Mater. Res.*, **16**, (2001).
5. Y. Liang, J.B. Rothman, and D.A. Bonnell, *J. Vac. Sci. Technol.*, **A12**, 2277 (1994).
6. R.C. Neville and C.A. Mead, *J. Appl. Phys.*, **43**, 4657 (1972).
7. H. Hasegawa and T. Nishino, *J. Appl. Phys.*, **69**, 1501 (1991).
8. G.W. Dietz, W. Antpohler, M. Klee, and R. Waser, *J. Appl. Phys.*, **78**, 6113 (1995).
9. T. Kawada, N. Iizawa, M. Tomida, A. Kaimai, K. Kawamura, Y. Nigara, and J. Jizusaki, *J. Euro. Ceram. Soc.*, **19**, 687 (1999).
10. S.M. Sze, in *Physics of Semiconductor Devices*, 2nd. ed. (Wiley, Singapore, 1981), p. 245.
11. J. Robertson, *J. Vac. Sci. Technol.*, **B18**, 1785 (2000).
12. A. Rothschild and Y. Komem, *Sensors and Actuators*, **B93**, 362 (2003).
13. T. Kawada, N. Iizawa, L.-Q. Han, K. Yashiro, A. Kaimai, Y. Nigara, and J. Mizusaki, in *Ionic and Mixed Conducting Ceramics IV*, *Electrochem. Soc. Proc.* edited by T.A. Ramanarayanan, W.L. Worrell, and M. Mogensen (The Electrochemical Society., Pennington, NJ, 2001) Vol. 2001–28.
14. L.-Q. Han, in "Characterization and modification of the surface and interface of SrTiO₃ based conductive materials," PhD thesis, Tohoku University, (2003).